Proceedings World Geothermal Congress 2020+1
Reykjavik, Iceland, April - October 2021

Application of Seismic and Geomechanical Approaches in Defining Geothermal Targets in the German Molasse Basin

Mohamed Fadel[a*], John Reinecker[b], Horst Kreuter[b]

[a] Leibniz Institute for Applied Geophysics (LIAG), Stilleweg 2, D-30655 Hannover, Germany

[b] Geothermal Engineering GmbH (GeoT), Baischstrasse 8, D-76133 Karlsruhe, Germany

*Corresponding author: mohamed.fadel@leibniz-liag.de

Keywords: Upper Jurassic carbonates, 3D seismic analysis, seismic attribute analysis, Molasse Basin, geothermal exploration, geomechanics, borehole breakout analysis, reef interpretation, karstification

ABSTRACT

Geothermal energy exploitation of the Upper Jurassic carbonates underlying the South German Molasse Basin is challenging due to its heterogeneous geological and structural characteristics (karst, fault zones, fractures, and lithofacies). Our approach is based on analyzing depth migrated 3D seismic data for mapping reef growth and areas of intensified karstification, as well as borehole data for correlation and calibration. A 3D facies model created by three seismic attributes displays the distribution of chaotic/massive and laminated/bedded facies of the Upper Jurassic carbonates. Geomechanical-geometrical considerations constrain the in situ stress state and the maximum horizontal stress orientation which found to be matching with the regional in situ stress field and observed open fracture orientation. The integration of these methodologies minimizes exploration risks related to the heterogeneous permeability distribution within the Upper Jurassic carbonates. They derive their validity from nearby projects results, well data, and geological observation, where the ease of their application decreases the overall exploration costs for the development of geothermal projects in the Molasse Basin.

1. INTRODUCTION

Thermal water (brine) properties such as: density, specific heat capacity, and salt content as well as production rate and temperature are the main controlling parameters for the success of any geothermal project (Schulz et al., 2007). With respect to low enthalpy geothermal exploitation, the Upper Jurassic carbonates of the South German Molasse Basin stands out as one of the main hydrothermal reservoirs in Europe. It accommodates a 300-600 m thick fractured-karstified carbonate reservoir, which is capable of producing 70-150 l/sec low salt content brine with temperatures of 80 to 140 °C from depths between 2500 and 4000 m (Agemar et al., 2014b; Mayrhofer et al., 2013). Such potential attracted district heating and power generation applications in Bavaria during the last decade.

The matrix permeability of the Upper Jurassic carbonates is low, where recent exploration campaigns in the Molasse Basin have failed due to encountering impermeable zones (ex: Geretsried, Mauerstetten, and Icking). However, its permeability may be enhanced by its geological (reefs lithofacies and diageneses), structural (karstification along faults) and geomechanical (open fracture network) characteristics (Homuth et al., 2015). Various geomechanical and seismic approaches have been suggested to characterize permeable targets within the Upper Jurassic carbonates. 3D seismic data and their attributes have been utilized in exploring reefs and karst systems (Lüschen et al., 2014; von Hartmann et al., 2012). Others have pointed out the importance of analyzing the permeability behavior of the E-W oriented faults zones (Moeck et al., 2015; Rojas et al., 2017; Mraz et al., 2018). Seithel et al. (2015) have emphasized the importance of applying geomechanical approaches in defining the structural permeability of the Upper Jurassic carbonates.

The Upper Jurassic carbonates deposited in the South German Jurassic Sea on a broad epicontinental passive shelf with a direct connection to the Tethys Ocean in the south (Meyer and Schmidt-Kaler, 1989). Two distinct facies of the Upper Jurassic carbonates are capable of being differentiated in the field and seismic surveys: massive (sponge and coral reefs and reef debris deposition) and bedded (basin and lagoon deposition) (Wolfgramm, 2012; Pawellek and Aigner, 2003; Meyer, 1994; Meyer and Schmidt-Kaler, 1989). Coral reefs (with high diversity) and siliceous sponge reefs were the main reef types evolved during the Upper Jurassic. In deeper waters between Late Oxfordian and Late Kimmeridgian, the sedimentation rate was low, where siliceous sponge meadows and mudmounds composed of microbial crusts and carbonate muds have flourished. Between Early to Late Tithonian, the water level dropped, increasing the sedimentation rate, which flourished reef growth and increased its deposition (Leinfelder, 2001). Translating this description into potential reservoir quality (primary permeability), the Tithonian coral reefs and debris are considered to be of a higher quality than the Kimmeridgian sponge reefs. Consequently, this study focuses on the Tithonian formation where high primary permeability is expected.

We present a methodical approach to explore optimal geothermal drilling targets by mapping the areas of increased permeability within early-late Tithonian. Two structural models based on depth 3D seismic data is introduced for the purpose of mapping possible reef and karst structures. Three seismic attributes are correlated with locations of massive facies (accommodating high permeability) interpreted from geophysical borehole data to create a 3D facies model which qualitatively analyzes interpreted structures. Borehole breakouts (BOs) are interpreted from image logs of highly deviated wells, where their orientation have been determined. A geomechanical-geometrical approach utilizes the BOs orientation in constraining the in situ stress state and the maximum horizontal stress (SHmax) orientation. The integration of these approaches yielded an exploration map used in defining prospective drilling targets for foreseen wells.

2. METHODS

2.1 Seismic Structural Analysis

2.1.1 Paleotopography evaluation

We start our approach by analyzing the paleotopography of the Early Upper Jurassic sequences. The objective is to obtain insights over the probable depositional locations of reefs and their debris. Early Oxfordian is the basement of the Upper Jurassic carbonates which is characterized by its strong seismic reflection in comparison with the absence of layering within the Upper Jurassic carbonates. We analyze its paleotopography to pinpoint locations of high elevation (paleohighs). This process sets an expectation for the distribution of reefs within Middle Kimmeridgian to Late Tithonian; especially the Tithonian coral reefs that flourished in shallow warm water (Leinfelder, 2001; Meyer and Schmidt-Kaler, 1989).

2.1.2 Reef Interpretation

Coral reefs had flourished between Early to Late Tithonian forming framestones of massive structures from several meters to 100 m (Leinfelder, 2001; Meyer and Schmidt-Kaler, 1989; Gwinnner, 1976, Paulsen, 1964). Figure 1.a shows a conceptual model for delineating coral reefs within Early-Late Tithonian. Increased thickness overlaid by anticline shaped sediments are interpreted as reef structures. These structures are then plotted on a map and compared with the location of paleohighs. The following steps illustrates the mapping process:

I. Creating thickness map of Early-Late Tithonian
II. Mapping increases in thickness
III. Analyzing morphology of overlain sediments (Top Purbeck)

2.1.3 Karst Interpretation

Circular collapse structures within the Upper Jurassic carbonates are indicators of sinkholes (karst structures) and can be mapped using 3D seismic data. They have developed due to the dissolution of Early-Late Tithonian formation. In order to explore these structures, a karst model is introduced in Figure 1.b. Top Purbeck, Early Tithonian, and Late Tithonian horizons are simultaneously utilized where: Top Purbeck represents the morphology of the overlain sediments, Early and late Tithonian horizons represent the reservoir section where dissolution took place developing collapse structures. Comparing the morphology of these horizons with respect to locating collapse structures would indicate locations of possible karst systems.

2.2 Seismic Attribute Analysis

Amplitude, variance and structural dip are the three utilized seismic attributes in creating a facies model (AVD model) representing the Upper Jurassic carbonates facies. Each of the mentioned attribute is correlated with geophysical borehole data. Table 1 describes the response of each of the attributes to the Upper Jurassic massive carbonate facies. The information in Table 1 is then transferred into one model by using the open source Fingerprint feature in OpendTect. It compares how similar is spatial data in a 3D cube with defined values (in our case here it compares the 3D seismic attributes data to the defined response of massive facies). It creates a 3D model scaled from 0-1: 0 represents laminated seismic facies (spatial data is not matching with the massive facies response) and 1 represents chaotic seismic facies (matching with the massive facies response). Finally, the AVD model is superimposed on the Late Upper Jurassic depth slices and is integrated with the results of the structural seismic analysis.

Table 1: Response of the picked attributes to massive permeable carbonate facies

Attribute	1- Amplitude	2- Variance	3- Dip
Response	Very low positive and negative magnitudes	High variance magnitudes	High dipping magnitudes

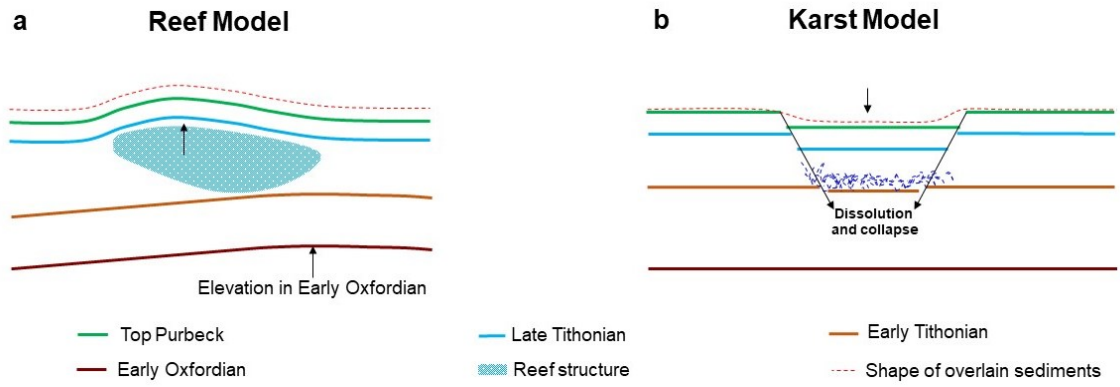

Figure 1: Conceptual reef and karst models applied in interpreting reef and karst structures within the reservoir.

2.3 Geometrical Geomechanical Analysis

The purpose of this approach is to constrain the stress regime and the orientation of the SHmax based on BOs orientation of highly deviated wells. Zoback (2007) had already introduced a mathematical approach to solve this problem. Here we apply a geometrical methodology based on comparing the BOs orientation with nine reference cases created by Peška and Zoback (1995). These cases describe the spatial orientation of the breakouts at different azimuth and deviation of well paths at different stress regimes at defined

conditions. At least two image logs of two different wells within the region of interest is required to apply this method. In order to utilize the reference plots geometrically these steps were followed:

I. Obtaining the magnitudes of the vertical stress (Sv) and the minimum horizontal stress (Shmin) from density logs and Leak-off tests respectively.
II. Defining the dominating stress between Sv and Shmin in order to eliminate four out of nine cases of Peška and Zoback (1995).
III. Interpreting the BOs from image logs, or from oriented caliper logs.
IV. Plotting the BOs on a stereographic projection following Peška and Zoback (1995).
V. Comparing and analyzing the plotted BOs of the wells with the five cases. Based on this step the orientation of the SHmax and the faulting stress regime can be constrained.

3. RESULTS

3.1 Seismic Structural Analysis

Figure 2 displays mapped paleohighs in Early Oxfordian horizon. Even though the Upper Jurassic formation is dipping by 3-4° southwards, the mapped paleohighs express a southward expansion that refer to their original elevation. Increased thickness (Mound bodies) of Early-Late Tithonian formation is observed around the paleohighs matching with the reef model shown in Figure 1. Figure 3.b displays those mound bodies, where the morphology of Top Purbeck (Figure 3.a) is evaluated. Coinciding anticline shaped sediment overlaying mound structures are interpreted as reefs and mapped in Figure 3.c. Coinciding deep centered bodies in Early Tithonian, Late Tithonian, and Top Purbeck horizons resulted in mapping karstificed structures (Figures 4 a, b, c, and d). Some of the karst structures in Top Purbeck were found to be divided into smaller ones in Early and Late Tithonian. Moreover, many of them are found around the vicinity of fault zones.

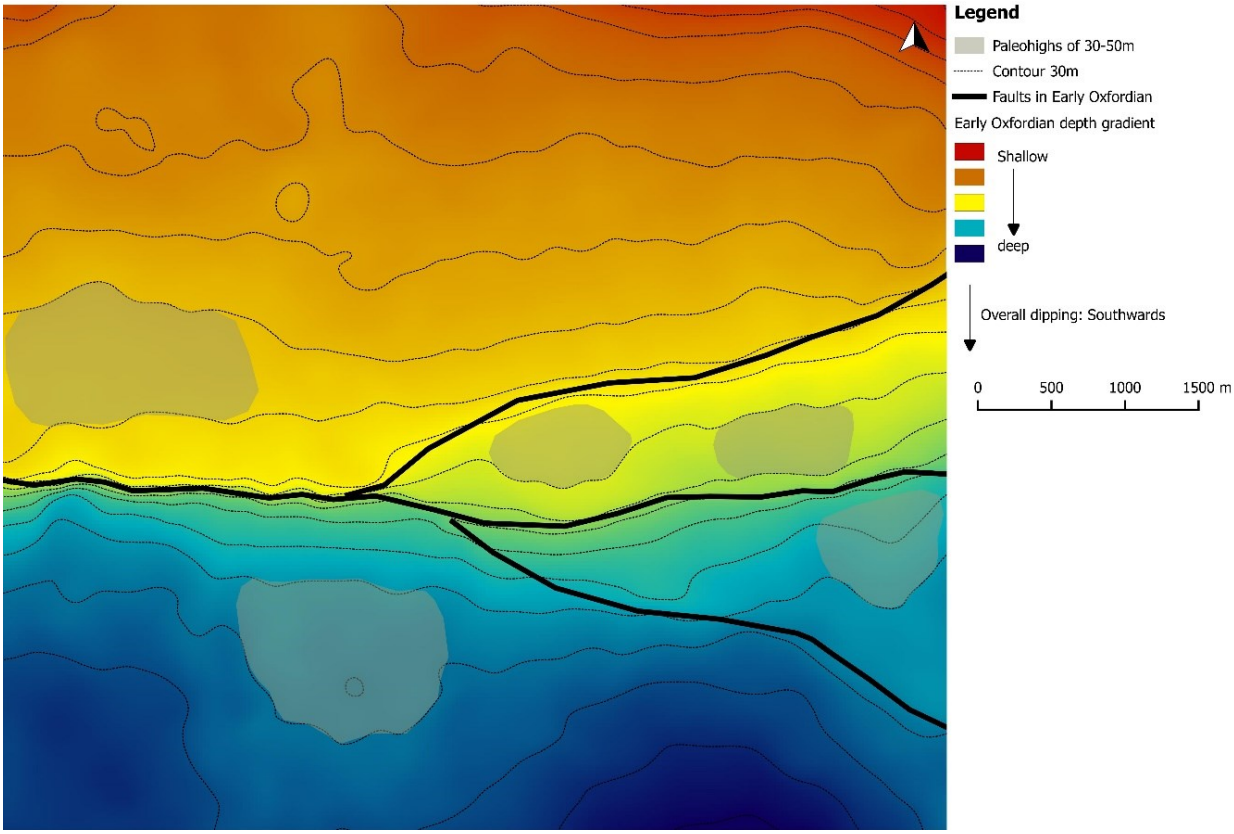

Figure 2: Picked paleohighs of 30-50 m elevation in Early Oxfordian.

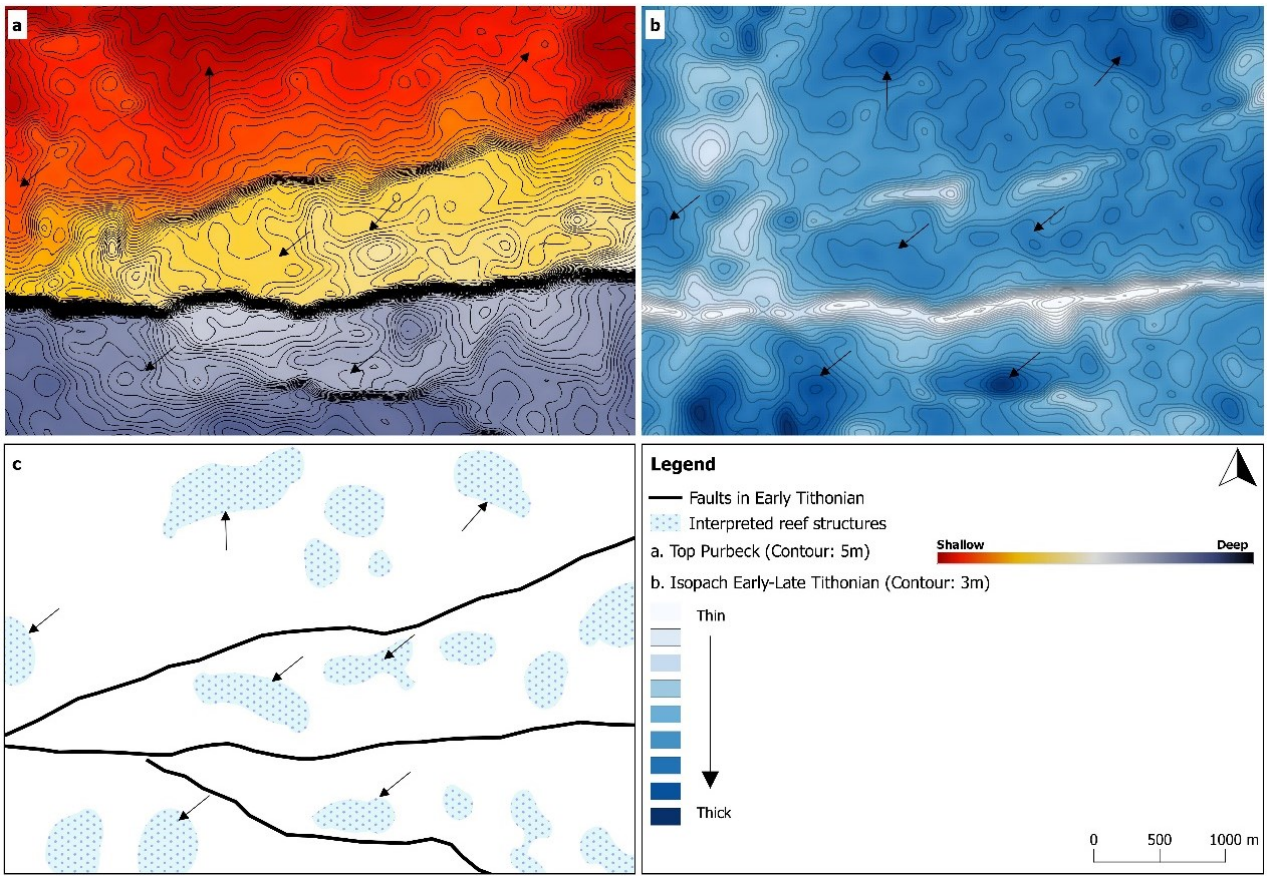

Figure 3: Mapping reef structures by comparing a-Top Purbeck with b-thickness map of Early-Late Tithonian.

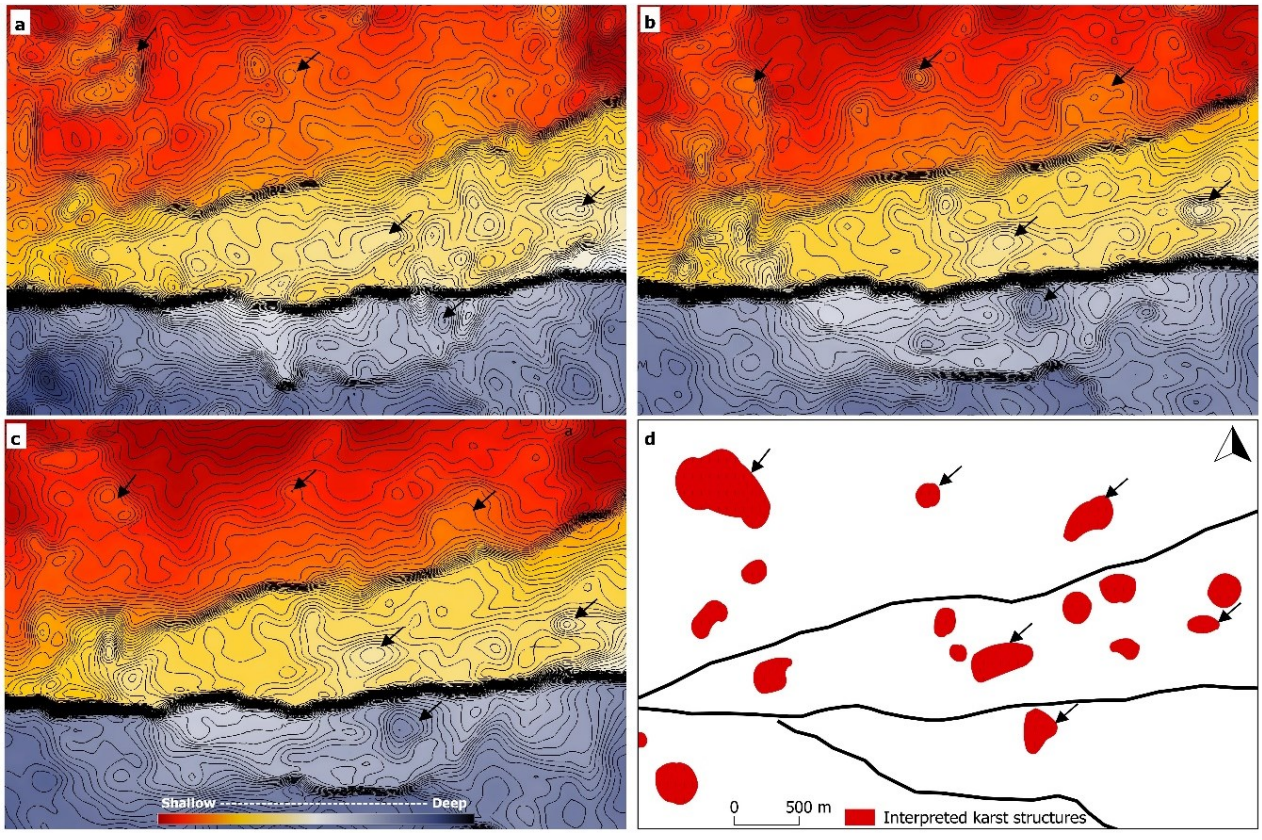

Figure 4: Mapping karst structures in the Upper Jurassic carbonate by analyzing a-Early Tithonian, b-Late Tithonian, and c-Top Purbeck.

3.4 Seismic Attribute Analysis

Figures 5 a, b, c, d and e display the main late Upper Jurassic horizons superimposed by the AVD model. Early Oxfordian is dominated by laminated seismic facies. There is a gradual increase in the chaotic seismic facies from Early Kimmeridgian to Late Tithonian. Top Purbeck accommodates many laminated facies, where the chaotic facies represent an eroded surface. The behavior of the seismic attributes signatures around fault zones express similar behavior to the chaotic facies, where fault zones accommodate: low magnitudes of amplitude, and high magnitudes of variance and dipping, where they can be spotted on every depth slice.

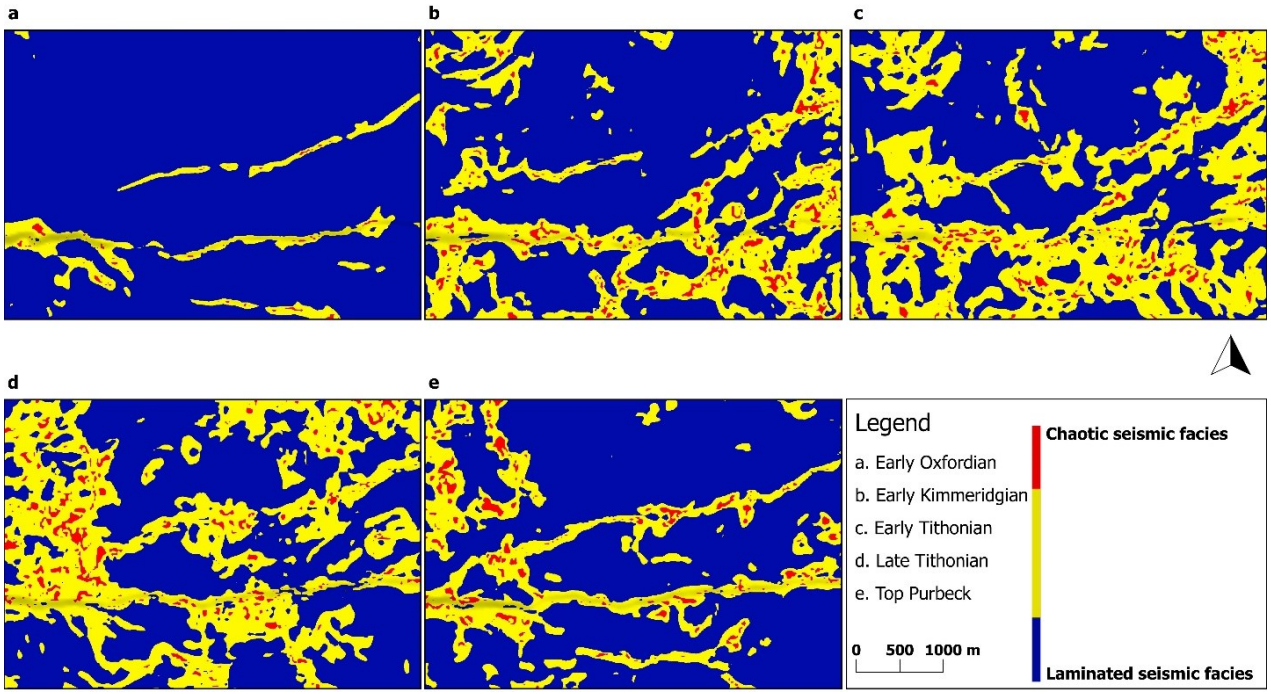

Figure 5: Upper Jurassic horizons superimposed by the AVD model. Notice the evolution of the chaotic seismic facies between b, c and d compared to a and e.

3.5 Geometrical Geomechanical Analysis

By comparing the magnitude of Sv and Shmin, it was found out that the Sv is the dominating one. That excludes the reverse faulting regime, where the rest of the analysis is applied on the five cases shown in Figure 6. The BOs were interpreted in the reservoir section from the image logs of two highly deviated wells, and were plotted on a stereographic projection (Figures 7.a and 7.b). The BOs in Figure 7.a are oriented towards the top and the bottom of the wellbore section where the well has a deviation of 90° and an azimuth of 130°. The BOs in Figure 7.b appears on the sides of the wellbore section, where the well has a deviation between 30° to 70° and an azimuth of 55°.

The orientation of the BOs in the first well in Figure 7.a is similar to case 5, indicating a strike slip faulting regime. Note that at a deviation of 90° in case 5: changing the orientation of SHmax will not change the orientation of the BOs, as they always appear at the top and bottom of the wellbore section at any azimuth. This confirms a strike slip faulting regime, where more analysis is required to confirm the orientation of the SHmax.

The BOs orientation of the second well in Figure 7.b is matching with cases 1 and 2 in Figure 6 of the normal faulting regime. Based on the strike slip faulting regime confirmation, the orientation of SHmax is suggested to be nearly parallel to the azimuth of the second well, where the effectiveness of SHmax around wellbore section is minimum. Therefore, Sv and Shmin controlled the BOs' orientation giving an apparent BOs orientation matching the normal faulting regime as Sv > Shmin. To derive the orientation of SHmax, case 5 is rotated clockwise (Figure 7.c) until a match between the orientation of BOs in both wells and case 5 is achieved. Consequently, the strike of SHmax is 32°N.

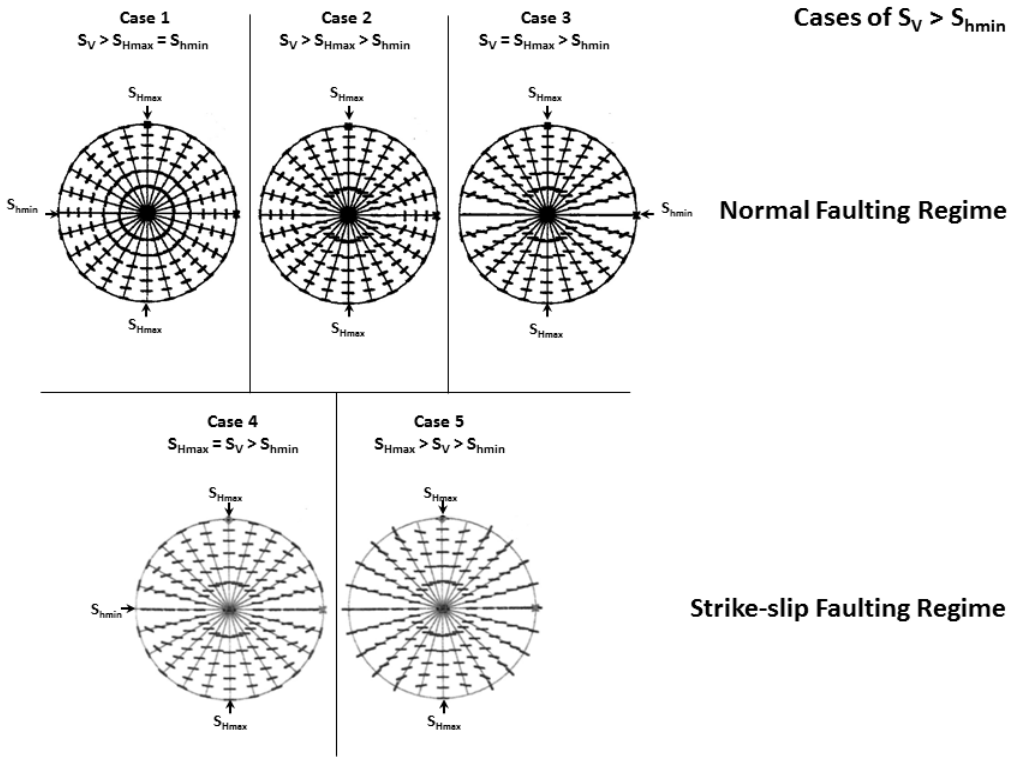

Figure 6:The five cases where Sv is > Shmin. Three cases from normal faulting regime and two cases from strike-slip faulting regime (Peška and Zoback, 1995). Note that case 5 is the only case whose BOs occurring at the top and bottom of the wellbore section at a deviation of 90° at any given azimuth.

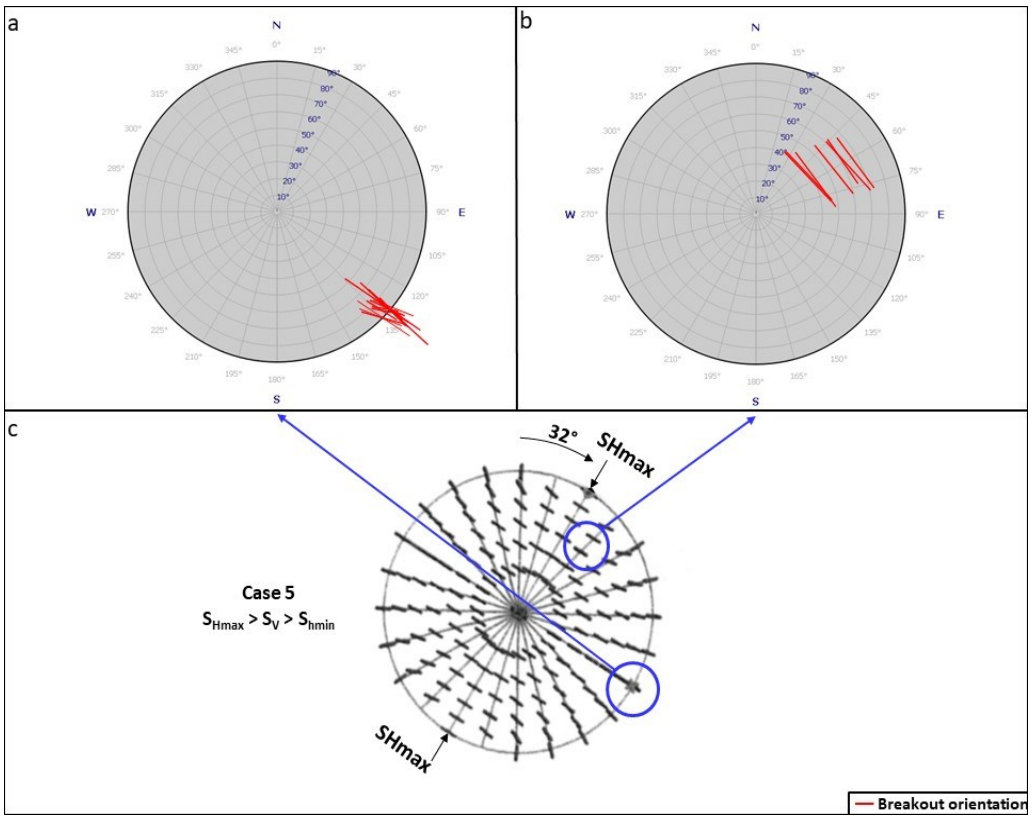

Figure 7: a and b display the orientation of the BOs of a horizontal (90° deviation) and a deviated well respectively. c displays the process of rotating case 5 (up to 32°) to match BOs orientation with the ones in a and b.

4. DISCUSSION

4.1 Structural seismic analysis

Water depth and paleotopography are the main controlling parameters of bathymetry, which had a direct influence on reef growth across the Upper Jurassic carbonate platform (Leinfelder, 1993a; Leinfelder, 1993b; Leinfelder, 2001). The sea level in the Late Upper Jurassic fluctuated between 50-100 m (Haq, 2017). Moreover, the absence of any tectonic activities as well as the slow sedimentation of carbonates maintained the topography of the paleohighs until Tithonian where corals flourished (Meyer and Schmidt-Kaler, 1996). Therefore, paleohighs of 30-50 m are expected to be a better habitat for coral reefs than the surrounding laminar platforms. Hence, picking paleohighs as well as analysing the morphology of the surrounding seismic reflectors are important for interpreting the location of coral reefs.

Increased sedimentation is a result from reef growth, which reflects abnormal increase in structural thickness of stratigraphic sequences. Chopra & Marfurt (2007) have listed two structural features of reef growth: increased thickness, and anticline shape of the overlain sediments. Taking into account the Upper Jurassic reef description, increased thickness in Tithonian refers to deposited corals and reef debris. Some of the mapped reefs are found around paleohighs from Early Oxfordian; matching the proposed reef model. Moreover, some of the mapped reefs intersected with wells within the study area. Points a, and c in Figure 8 show the positive correlation between bioherms interpreted from image logs and the mapped structures.

Karstification is one of the main key elements controlling the present-day permeability of the Upper Jurassic carbonates (Homuth et al., 2015). The evolution of karst systems depends on lithofacies (primary permeability), and are enhanced by structural permeability (fracturing and faulting). Primary permeability of Tithonian coral reef carbonates is better than that of Oxfordian and Kimmeridgian sponge reefs. Hence, the karst model mapped karst structures in Early-Late Tithonian formation, where their morphology represent sinkholes. They have similar morphology to the sinkholes detected in the Franconian Alb's outcrops and the circular structures interpreted by Lüschen et al. (2014). Figure 8 correlates the existence of karst from image logs with mapped karst structures from 3D seismic data. Karst structures in point d is positively correlated with karst facies shown in the image logs.

4.2 AVD Model

In our approach, the identification and determination of the areal extent of interesting structural features (reefs, karst, and fault zones) within the late Upper Jurassic carbonates have been supported with the utilization of seismic attributes. They are important indicators providing additional information sensitive to carbonate facies, which helps in picking optimum drilling targets (Chopra & Marfurt, 2007). The depth slices superimposed by the AVD model in Figure 5 exemplify the facies distribution of the late Upper Jurassic carbonates described by Meyer and Schmidt-Kaler (1989) where:

- Early Oxfordian is dominated by laminated seismic facies representing the slow sedimentation rate and the lack of reef growth.
- The evolution of chaotic seismic facies from Early Kimmeridgian to Late Tithonian representing the fast sedimentation rate of carbonates and the reef growth.

Figure 8 displays the Correlation between the AVD model and interpreted structures from 3D seismic with wells data (mud losses and facies). Points c and d in Figure 8 show the positive correlation between the chaotic seismic facies described by the AVD model and mud losses. Point b represents a laminated seismic facies interval which coincides with impermeable zones represented by low mud losses. The existence of chaotic seismic facies in point a, reflects a tendency of the mud losses to increase.

The Reliability of utilizing the AVD model singularly is not recommended, as it should be associated with interpreted structures following the presented approaches. Interpreted chaotic seismic facies from the AVD model that coincides with interpreted reef or karst structures are often associated with an increase in mud losses (points a, c, and d, in Figure 8). Point b is an impermeable zone that represent an interpreted karst structure associated with low values of AVD model. As a result, the utilization of the AVD model in interpreting permeable zones is valid under the condition that it is positively correlated with structures.

4.3 Geometrical Geomechanical Analysis

The observed faulting regime from the presented approach coincides with regional and local observations where:

- Illies and Greiner (1978) and Lemcke (1988) proposed that the tectonic regional setting of the Molasse Basin is compressional with SHmax being the dominating principle stress.
- Reinecker et al. (2010) concluded from borehole observations throughout the South German Molasse Basin that the present-day stress is most likely strike-slip to reverse faulting regime.
- Seithel et al. (2015) performed a study based on frictional equilibrium theory on data from Sauerlach, where at 4 km depth strike-slip regime prevails.
- Ziegler et al. (2016) from 3D stress field modelling of the Munich area proposed that within the Upper Jurassic carbonates a strike slip faulting regime prevails.

Figure 9 displays the SHmax orientation derived from this study and the ones derived by Reinecker et al.2010. It is obvious that the SHmax orientation of the southern wells in Figure 9 acts N-S, while the northern wells have a deflected towards NNE-SSW. Moreover, the average strike orientation of 741 interpreted partial open fractures from Image-logs of the project's wells (shown in Figure 9) is 27°N. Hence, the applied methodology for deriving the orientation of SHmax is representative and can provide acceptable indications on the orientation of the SHmax. However, this methodology cannot be used in deriving the magnitudes of the stress tensors.

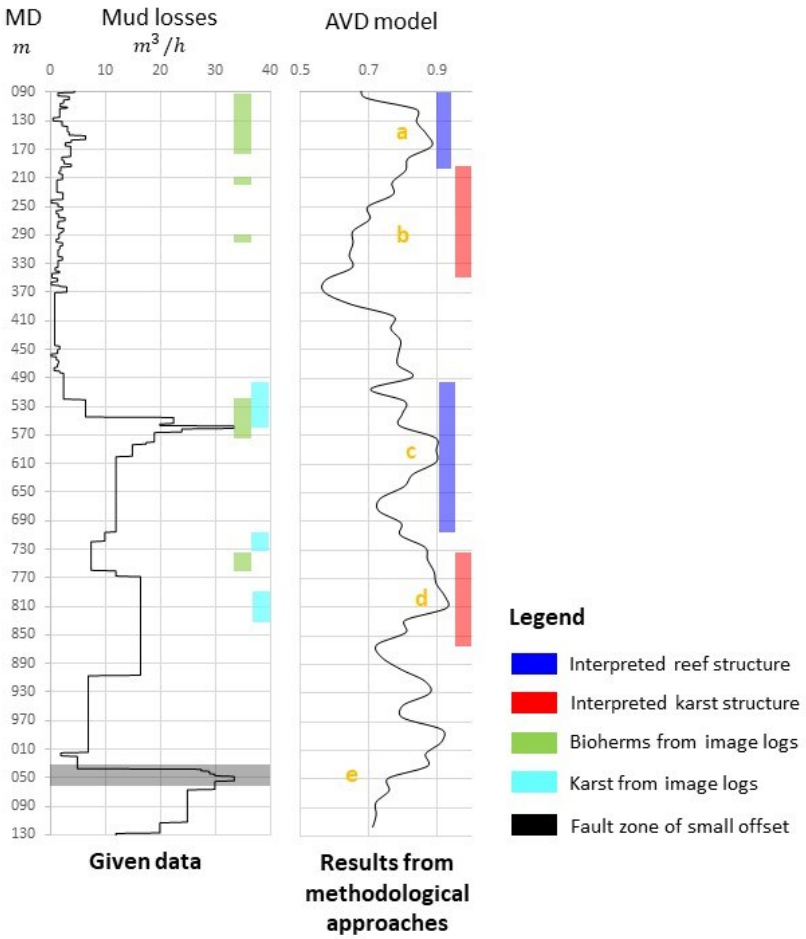

Figure 8: Correlation between given well data (drilling mud losses and interpreted facies from image logs), AVD model (high values represent chaotic seismic facies), and mapped structures from proposed approaches (reefs and karst) of a well in the study area.

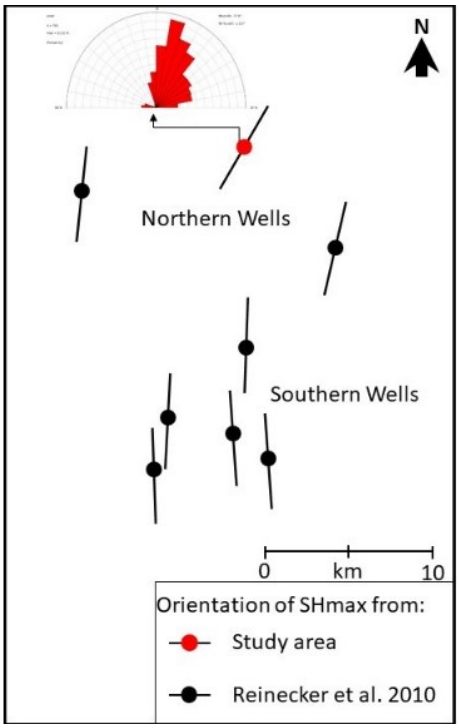

Figure 9. Comparing the derived orientation of SHmax (in red) with nearby wells (in black) from Reinecker et al. (2010). Notice the tendency of the northern wells to be deflected NNE-SSW (similar to the findings of this study) compared with the Southern wells.

4.4 Integration of Methods

Figure 10 displays an example of the exploration map constructed to find optimal drilling targets in the Upper Jurassic carbonates. The plotted paleohighs, reefs, and karst structures define the areal extent of interesting structures. The chaotic seismic facies existing between Early-late Tithonian are plotted into the same map to qualitatively validate picking prospective drilling targets. Small displacement offset fault zones in the study area are associated with major mud losses (Figure 8) where large offset ones were found to be impermeable. It is believed that small offset fault zones accommodate high perpendicular permeability component due to low clay smear and the optimal juxtaposition of the massive facies of the Early-Late Tithonian formation (Figure 11).

The orientation of the SHmax influences mechanically the structural permeability behavior of the reservoir, where open natural and hydraulically induced fractures are found to be parallel to the SHmax (Zoback, 2007; Hubbert and Wellis, 1957). Faults in the study area of small displacement and strike of 10°-40° to the SHmax orientation have been proven being hydraulically active. They have a high slip tendency, which enhances the structural permeability along and across their strike. Hence, integrating fault zones and taking the influence of SHmax orientation into account is highly recommended.

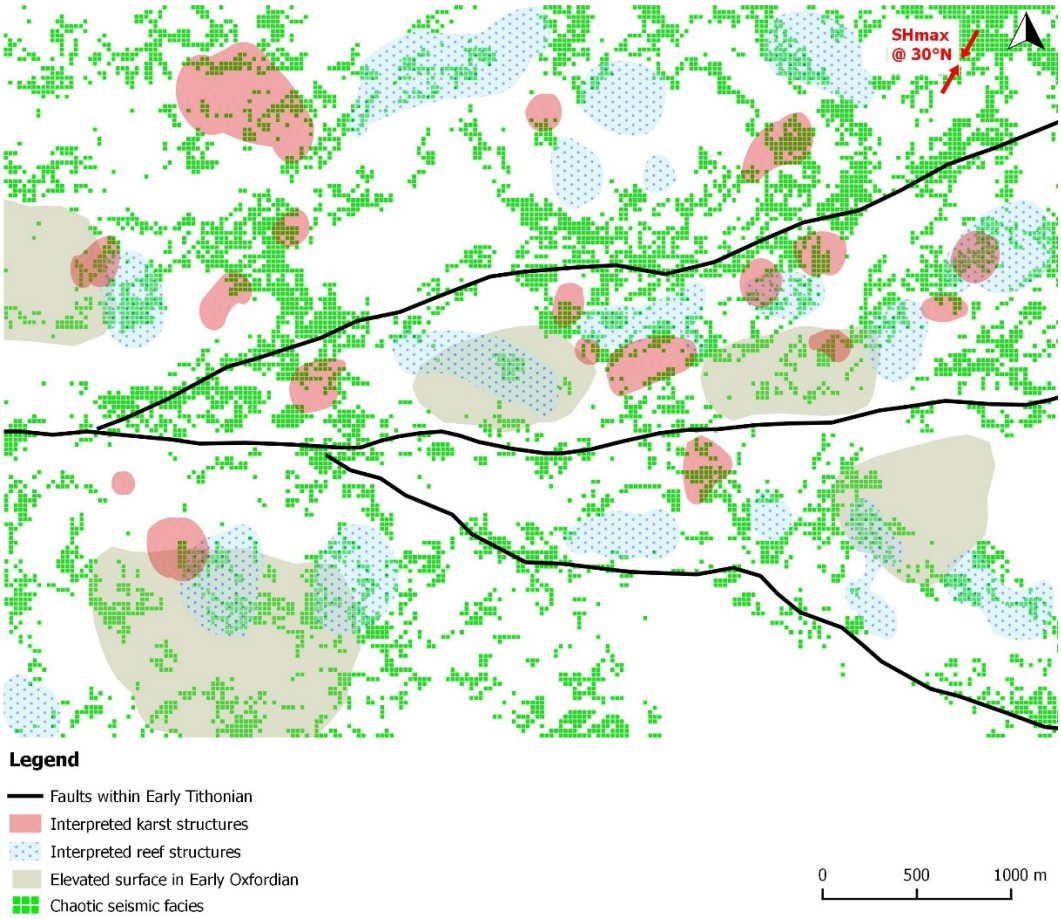

Figure 10: An example of the final exploration map used in defining drilling targets in the Upper Jurassic carbonates.

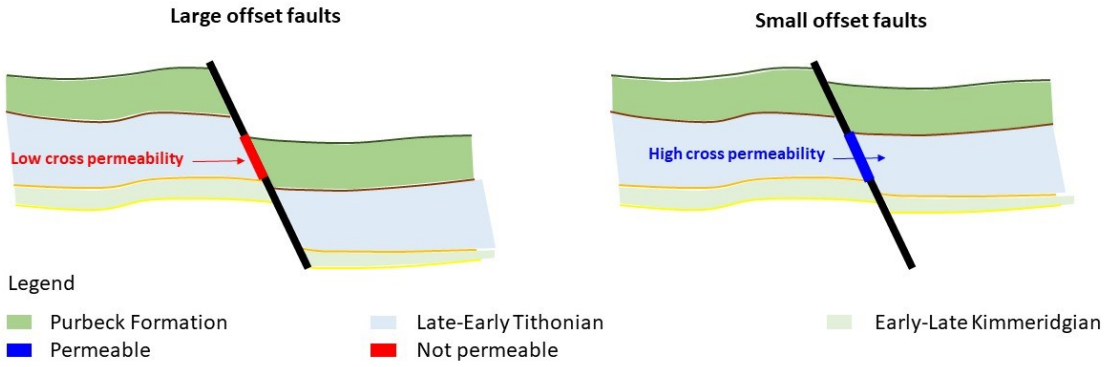

Figure 11: Small displacement faults are associated with major mud losses compared to large ones that act as structural traps.

5. CONCLUSIONS

In this study, we present a systematic approach to explore targets of interest in the Upper Jurassic carbonates of the South German Molasse Basin. The heterogeneity of the reservoir's permeability urges the importance of utilizing various methodologies to reduce exploration risks. Structural seismic analysis as well as the utilization of seismic attributes is capable of discriminating between the different carbonate facies. Location of interpreted reef and karst structures positively correlate with interpreted bioherms facies and karst from image logs respectively. Chaotic seismic facies along well paths within the 3D seismic cube often associate with high mud losses while drilling. Promising geothermal targets are characterized by structural features with chaotic seismic facies (for enhanced primary permeability) along fault zones (for hydraulic active fracture network and/or intensified karstification) and juxtaposition of massive facies along fault zones of minor offset (enabling valuable permeability across fault zone). Plotting the results into one exploration map helps the decision making of selecting prospective targets, where a combination of all the mentioned parameters is recommended. The results of the geomechanical-geometrical approach confirm a strike-slip faulting regime within the study area and a 32° N SHmax orientation. In comparison with other resources, those findings were representative where they confirm the validity of applying the introduced approach to find the SHmax orientation; however, not its magnitude.

Finally, the prospective wells should be designed to:

1. Penetrate structural features within Early-Late Tithonian that accommodate chaotic seismic facies.
2. Exploit fault zones of minor offsets and of strike nearly parallel to SHmax orientation.
3. Intersect optimal oriented fractures by optimizing well path azimuth and deviation against SHmax orientation.

6. REFERENCES

Agemar, T., Weber, J., and Schulz, R.: Deep geothermal energy production in Germany, *Energies*, (2014b), 4397-4416.

Chopra, S., and Marfurt, K.:Seismic Attributes for Prospect Identification and Reservoir Characterizatio, OK U.S.A, *Society of Exploration Geophysicists*, (2007).

Gwinner, M. P.: Origin of the Upper Jurassic limestones of the Swabian Alb (Southwest Germany), *Contr. Sedimentol,* (1976), 5:1-75.

Haq, B. U.: Jurassic sea level variations: A reappraisal, *GSA TODAY, V. 28,* (2017).

Homuth, S., Götz, A., and Sass, I.: Reservoir characterization of the Upper Jurassic geothermal target formations (Molasse Basin, Germany): role of thermofacies as exploration tool, *Geothermal Energy Science,* 3, (2015), 41-49.

Hubbert, M., and Willis, D.: Mechanics of Hydraulic Fracturing, *Transactions of Society of Petroleum Engineers of AIME, 210,* (1957), 153-163.

Illies, J. H., and Greiner, G.: Rhinegraben and the Alpine system, *GSA Bul, 89,* (1978), 770-782.

Leinfelder, R. R.: A sequence stratigraphic approach to the Upper Jurassic mixed carbonate-siliciclastic succession of the central Lusitnian Basin, Portugal, (1993b), Profil 5:119-140.

Leinfelder, R. R.: Upper Jurassic Reef Types and Controlling Factors.-A preliminary report, s.l., (1993a), Profil 5:1-45.

Leinfelder, R. R.: Jurassic Reef Ecosystems. In: The History and Sedimentation of Ancient Reef Systems, New York: *Kluwer Academic / Plenum Publishers*, (2001), 251-309.

Lemcke, K.: Das Bayerische Alpenvorland vor der Eiszeit, Stuttgart, *Schweizerbart Science Publishers*, (1988).

Lüschen, E., Wolfgramm, M., Fritzer, T., Dussel, M., Thomas, R., and Schulz, R.: 3D seismic survey explores geothermal targets for reservoir characterization at Unterhaching, Munich, Germany, *Elsvier, Geothermic 50,* (2014), 167-179.

Mayrhofer, C., Niessner, R. and Baumann, T.: Hydrochemistry and hydrogen sulfide generating processes in the Malm aquifer, Bavarian Molasse Basin, Germany, *Hydrogeology Journal, 22,* (2013), (1).

Meyer, R. K. F.: die erste Kernbohrung durch den Malm unter der bayerischen Molasse, *Erlanger geol. Abh., 123*, (1994), 51-81.

Meyer, R. K. F. and Schmidt-Kaler, H.: Paläogeographischer Atlas des süddeutschen Oberjura (Malm), Stuttgart: *Schweizerbart*, (1989).

Moeck, I., Uhlig, S., Loske, B., Jentsch, A., Ferreiro Mählmann, R., and Hild, S.: Fossil Multiphase Normal Faults -Prime Targets for Geothermal Drilling in the Bavarian Molasse Basin?*, Proceedings,* World Geothermal Conference, Melbourne, Australia, (2015).

Mraz, E., Moeck, I., Bissmann, S., and Hild, S.: Multiphase fossil normal faults as geothermal exploration targets in the Western Bavarian Molasse Basin: Case study Mauerstetten, *Z. Dt. Ges. Geowiss. 169*, (2018), 389-411.

Ortiz Rojas, A. E., Dussel, M., and Moeck, I.: Borehole geophysical characterisation of a major fault zone in the geothermal Unterhaching Gt 2 well, South German Molasse Basin, *Z. Dt. Ges. Geowiss. 169,* (2017) 445-463.

Paulsen, S.: Aufbau und Petrographie des Riffkomplexes von Arnegg im höheren Weoßen Jura de Schwäbischen Alb (Wurttemberg), Arbeiten aus dem Institute für Geologie und Paläontologie der Universität Stuttgart, *NE 42,* (1964) 1-98.

Pawellek, T., and Aigner, T.: Apparently homogenous "reef"-limestones built by high-frequency cycles: Upper Jurassic, SW-Germany, *Sedimentary Geology 160, (*2003), (s 1–3):259–284.

Peška, P. and Zoback, M. D.: Compressive and tensile failure of inclined well bores and determination of in situ stress and rock strength, *Journal of Geophysical Research: Solid Earth, 100(B7),* (1995), 12791-12811.

Reinecker, J., Tingay, M., Müller, B., and Heidbach, O.: Present-day stress orientation in the Molasse Basin, *Elsevier, Tectonophysics 482,* (2010), 129-138.

Schulz, R., Agemar, T., Alten, A. J., Kühne, K., Maul, A. A., Pester, S., and Wirth, W.: Aufbau eines geothermischen Informationssystems für Deutschland, Volume 123, (2007), 76-81.

Seithel, R., Steiner, U., Müller, B., Hect, C., and Kohl, T.: Local stress anomaly in the Bavarian Molasse Basin, *Geothermal Energy 3, Article number 4,* (2015).

von Hartmann, H., Buness, H., Krawczyk, C., and Schulz, R.: 3-D seismic analysis of a carbonate platform in the Molasse Basin - reef distribution and internal separation with seismic attributes, *ELSEVIER, Tectonophysics ,*(2012), 572-573.

Wolfgramm, M., Dussel, M., Lüschen, E., Schulz, R., Thomas, R., and Koch, R.: Untersuchungen des geothermischen Hauptgrundwasserleiters im süddeutschen Molassebecken, *bbr Sonderheft,* (2012), 75-82.

Ziegler, H., Reinecker, J., Przybycin, A. and Scheck-Wenderoth, M.: A multi-stage 3-D stress field modelling approach exemplified in the Bavarian Molasse Basin, *Solid Earth 7,* (2016), 1365-1382.

Zoback, M. D.: Reservoir Geomechanics, *California: Cambridge University Press*, (2007).